Modeling and Fault Diagnosis of a Polymer Electrolyte Fuel Cell Using Electrical Equivalent Analysis

Andres Hernandez, Daniel Hissel, *Senior Member, IEEE*, and Rachid Outbib

***Abstract*—Fuel cell systems are complex systems and a high degree of competence is needed in different areas of knowledge such as thermodynamics, fluid dynamics, electrochemistry, and others, for their comprehension. This paper is a contribution to global modeling and fault diagnosis of these systems. More precisely, the goal of this paper is twofold. First, an electrical equivalent model, which could be used as a unifying approach to fuel cell systems will be resented. Second, a methodology to use the electrical model for fuel cell system diagnosis will be introduced, making special emphasis on fuel cell flooding detection. In order to illustrate the relevance of the proposed approach, experimental validations of the model, and the diagnosis methodology are proposed.**

***Index Terms*—Equivalent electrical circuit, flooding, fuel cell, fuel cell diagnosis, modeling.**

NOMENCLATURE

D	Electroosmotic drag coefficient
H_r	Relative humidity
I	Current (A)
l	Length (m)
m	Mass (kg)
M	Molar mass (kg/mol)
n	Number of moles
N	Number of cells
P	Pressure (Pa)
Q	Molar flow (kg/s)
R	Ideal gas constant, resistance
T	Temperature (K)
v	Volume (m^3)
V	Voltage (V)
α	Electron exchange
μ	Density (kg/m^3)
Subscript	
atm	Atmospheric conditionsx
f	fluid
in	input
l	load
m	molar
M	mass
oc	open circuit
out	output
s	stack
vap	Vaporized
Superscript	
a	anode
c	cathode
m	membrane

Manuscript received July 14, 2008; revised July 18, 2008. First published December 15, 2009; current version published February 17, 2010. Paper no. TEC-00350-2006.

A. Hernandez and D. Hissel are with the Laboratory of Electrical Engineering and Systems (L2ES), University of Franche-Comte, Belfort Cedex 90010, France (e-mail: andres-ignacio.hernandez@utbm.fr).

R. Outbib is with the Laboratorie des Sciences de l'Information et des Systemes (LSIS), University of Aix-Marseille II, Domaine Universitaire de Saint Jérôme, 13397 Marseille Cedex 20, France.

Color versions of one or more of the figures in this paper are available online at http://ieeexplore.org.

Digital Object Identifier 10.1109/TEC.2009.2016121

I. INTRODUCTION

FUEL cells are promising and environmentally friendly energy conversion devices. Indeed, fuel cells have a theoretical efficiency higher than the one offered by thermal machines, suggesting that an eventual replacement of combustion technology by a more efficient electrochemical conversion is feasible. However, fuel cell technology is not sufficiently developed to provide energy at competitive costs and a considerable effort is still required to optimize its performance, reliability, and life time, in order to reduce their production and exploitation costs. In the pursuit of these goals, engineers interested on fuel cell applications, require friendly representative models of fuel cells that could provide both: an easy approach and a rapid comprehension of involved technological principles, preserving a reliable prediction capacity in standard and extreme operating conditions [1]. An electric equivalent model fits many of these requirements [2]. Indeed, its schematic representation serves as common language to many disciplines, acting as interface model for multidisciplinary team work. As a matter of fact, this methodology is often used to model electrical machines and hydraulic networks (see for instance [3] and [4]). Some researchers have already used this approach to model gas behavior in polymer electrolyte fuel cell (PEFC) under specific operating conditions [2], [5]–[7]. Other authors have used electrical equivalent circuits to approach fuel cell diagnosis [8] from an electrochemical point of view. However, the proposed diagnosis approach is based on the analysis of gas dynamics to determine fuel cell equivalent electrical model changes. Additionally, this modeling and diagnosis approach allows the estimation of species concentration dynamics, which is a very useful information to determine fault origin.

This paper is a contribution to global modeling and fault diagnosis. The first goal of this study is to present a new global model based on electric equivalent for a PEFC. This new model takes into account the main nonlinearities of the process and it improves classical models in three ways. First, the proposed

model decouples gases onto their composing species allowing partial pressure calculations and species parameter dependence analysis. Second, this model extends predicting capabilities of existing models for various operating conditions, including water vapor saturation [9] and other nonlinearities associated to fluid dynamics. Third, this model includes also additional nodes for the membrane and diffusion layers, making it suitable for prediction under diphasic water conditions.

The second goal of this study is to use this new model in order to establish results on fault diagnosis.

The paper, which is divided into eight sections, is organized as follows. The second section is dedicated to a short description of a typical fuel cell system. In the third section, an introduction to the modeling approach is presented. In the fourth section, the fuel cell system model is introduced, making special emphasis on the stack. In the fifth section, the parameter identification method is detailed. Afterwards, the model validation through simulation and experimental results for tests done on a 500W PEFC test bench are presented. In the seventh part, fuel cell diagnosis methodology is introduced and experimental validation for the proposed methodology is presented for flooding failure. The last section will be dedicated to conclusions and perspectives.

II. Fuel Cell System Description

In fuel cells, the electrochemical reaction sets a typical nominal mean load voltage of 0.7 V between electrodes.

In order to accomplish higher voltages, it is necessary to stack several basic cells connected in an electrical serial configuration and feed them in a parallel way. The cell is fed continuously with fuel on the anode side and with an oxidant on the cathode side. Water is a by-product of the electrochemical reaction. In low-temperature fuel cells (such as PEFC), protons are the charge carriers in the electrolyte. Theoretically, fuel cell efficiency is higher than the one of a thermal machine. However, in practice, the efficiency of the fuel cell system is actually diminished if we take into account the ancillary systems that consume part of the fuel cell energy. Other energy loses such as ohmic internal effects are also to be considered in calculating the overall efficiency of the fuel cell. Nevertheless, the fuel cell system remains more efficient than most thermal machines.

Focusing on PEFC stacks operated at low temperatures, hydrogen and oxygen are provided onto catalytic porous electrode plates, which are separated by an electrolyte membrane. In order to provide an adequate gas management, several additional ancillary circuits are needed as part of the fuel cell system: hydrogen circuit, air circuit, cooling circuit, and humidification circuit (see Fig. 1).

Many of fuel cell internal parameters such as diffusion constants, electroosmotic coefficients, and electrical resistances, are dependant on membrane and gas water contents [1], [10]. Thus, there is a particular interest on looking carefully to water and water vapor evolution and control. Notice that initial water vapor content is ensured by a humidifying system, which adds the adequate amount of vapor to air and/or hydrogen flows, in order to obtain the required humidity level at stacks input nozzles [11], [12].

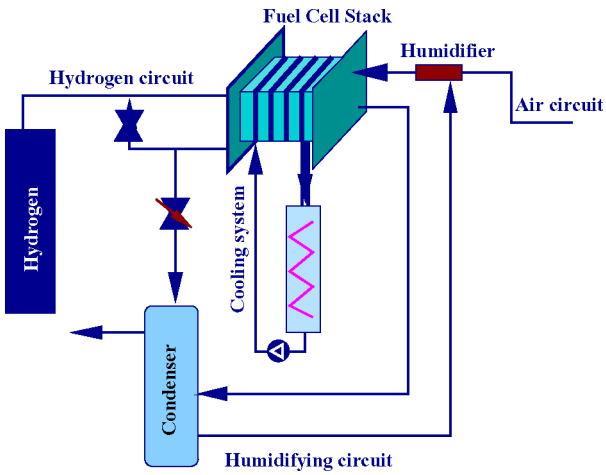

Fig. 1. System block schematic.

III. Modeling Approach

In classical physics, matter, charge, and energy are preserved. Kirchoff's node and loop laws are representations of those fundamental principles applied to network analysis. Generally speaking, these fundamental principles can be extrapolated to any network structure, including pneumatic and hydraulic networks [1], [3], [4], [5]–[7]. Considering this fact, an electric equivalent model is built, based on charge, matter, and energy conservation laws. In this approach, each component of an hydraulic or pneumatic circuit is represented by its electrical equivalent in an electric circuit.

Comparing the physical behavior of pneumatic elements with those of electrical circuits, an analogy between these two isomorph systems can be established to find the electrical equivalence of pneumatic systems.

Electrical current and fluid flows, share in their bases the same definition, and thus are expressed by similar mathematical expressions as seen on

$$\begin{aligned}\text{Electrical environment} &\left\{ I = \frac{dq}{dt} \right. \\ \text{Pneumatic environment} &\left\{ Q_{m,\text{net}} = \frac{dn}{dt} \right. \end{aligned} \tag{1}$$

where

$$Q_{m,\text{net}} = \sum Q_{m,\text{in}} - \sum Q_{m,\text{out}} \tag{2}$$

This makes electrical current an ideal equivalent variable for either mass or molar flow.

According to Bernoulli's continuity law, if a fluid is said to be incompressible, nonviscous, and following a laminar flow, the energy and mass flow are preserved when flowing through an ideal pipe. Under such considerations, the pneumatic conductor is assumed to behave as an ideal conductor (see Fig. 2).

Clearly, the mechanical losses produced by nonconservative forces are present in fluid flows. These losses are classically modeled by an empirical fluid equation known as Poiseuille's law [13]. This law states that for a laminar flow in an incompressible fluid, a proportional relation is established between pressure

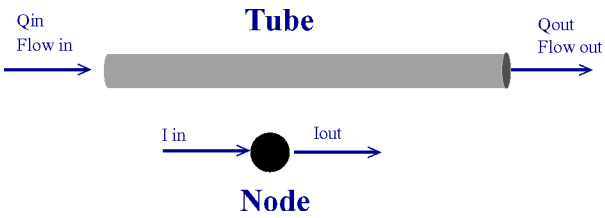

Fig. 2. Ideal tube model.

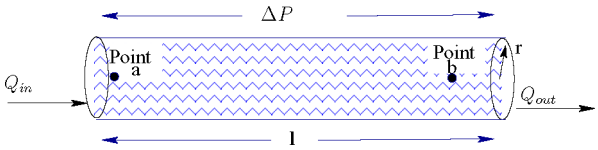

Fig. 3. Real tube associated with Poiseuille's law.

losses and flow. If the fluid viscosity is considered constant between points "a" and "b" (see Fig. 3), an equivalent between Poiseuille's law and Ohm's law can be easily expressed by

$$\text{Pneumatic environment} \left\{ Q_m = \Delta P \left(\frac{\pi r^2}{8 \mu l} \right) \right.$$
$$\text{Electrical environment} \left\{ I = \frac{\Delta V}{R_f} \right. \tag{3}$$

where r is the hydraulic radius and l is the tube length (see Fig. 3). Then, the pneumatic resistance can be taken as given by

$$\begin{cases} R_f \equiv \dfrac{8 \mu l}{\pi r^2} \\ \Delta P \equiv \Delta V. \end{cases} \tag{4}$$

Using (3), it can be deduced that voltage can be considered as an electrical equivalent variable for pressure. The hypothesis of having a constant equivalent pneumatic resistance R_f can also be assumed, if the validity constraints of Poiseuille's law are taken into account. In this study, even if pneumatic resistance is distributed uniformly trough all channel length, modeling is much easier if resistances are concentrated onto punctual resistances.

If a compressible fluid is taken into consideration, a variation of the fluid mass inside pipes can occur (i.e., $Q_{M,\text{net}} \neq 0$, $Q_{m,\text{net}} \neq 6 = 0$). In this case, the pneumatic conductor can no longer be modeled by a simple resistance, and a variable storage device should then be added to the model.

From the ideal gas law and assuming that temperature and volume are constant, the following equation can be deduced:

$$\frac{dP}{dt} = \frac{RT}{v} \frac{dn}{dt} \tag{5}$$

Considering molar flow definition

$$Q_m = \frac{dn}{dt} \tag{6}$$

the variation of pressure can be expressed by

$$\text{Pneumatic environment} \left\{ \Delta P = \frac{RT}{v} \int_t^{to} Q_m \, dt. \right. \tag{7}$$

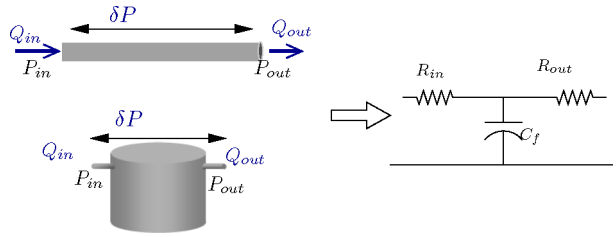

Fig. 4. Pneumatic component electric equivalent.

The previous equation can be considered as an isomorphism of the following equation, representing a capacitors voltage in a *RC* circuit

$$\text{Electric environment} \left\{ \Delta V = \frac{1}{C} \int_t^{to} I \, dt. \right. \tag{8}$$

A comparison between (7) and (8) will lead to define voltage as the natural electrical equivalent for pressure. Moreover, it is possible to introduce pneumatic capacitance concept C_f, using the following expression:

$$C_f \equiv \frac{v}{RT} \tag{9}$$

in complement to resistive properties described by (4).

After superposing both resistive and capacitive properties of pneumatic conductors in the same circuit, a resulting "T" quadripole model can be constructed as an electric equivalent for pneumatic conductors. Compared to other electrical equivalent models using a single resistance (see [6]), the "T" configuration (see Fig. 4) takes into account the differences between the input and output gas flows. This fact will allow time constant tuning of the proposed model, according to different flow and current profiles.

Other components of the fuel cell system (e.g., tanks, valves, etc.) can also be modeled by the same basic *RC* circuit under most operating conditions. While modeling tanks, a constant mean gas speed and a constant pressure can be considered inside the tank volume.

Experimentally found pressure drops (ΔP) between element input and output terminals (Figs. 9 and 10), will be modeled by means of input resistance (R_{in}) and output resistance (R_{out}) present on the *RC* circuit. These resistances found a theoretical support on nozzle equations [11], [12]. However, experimental data strongly suggest that gas flow and pressure drop follows a quadratic relation rather than the proportional relation presented in [12]. The quadratic pressure drop versus flow relation is considered in the model. Summarizing, in this model all components having a nonnegligible volume are decoupled onto three parts.

1) The first part consists in modeling the volume, by a pneumatic capacitance C_f.
2) The second one deals with the input nozzle, modeled by an input resistance R_{in}.
3) The last one concerns the output nozzle represented by an output resistance R_{out}.

All pressure drops are concentrated on component nozzle [11], [12].

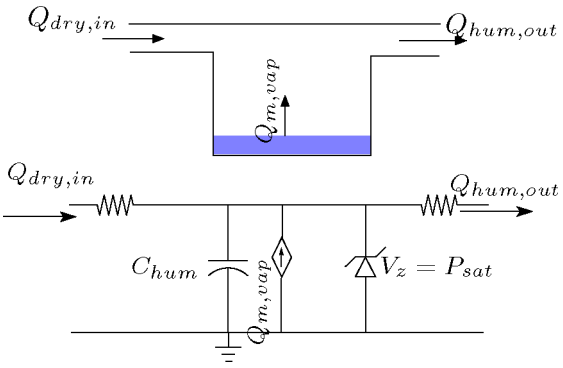

Fig. 5. Electric equivalent circuit for humidifier.

IV. Fuel Cell Model

The next step in our modeling procedure is to join the previous models, in order to obtain a representative electrical equivalent circuit for the fuel cell system.

A. Input Gas System

This system is composed mainly by pipes, regulation valves and a humidifying system [11]. All components are modeled by an *RC* quadripole as described in last section. The interconnectivity between components will lead to a single equivalent *RC* circuit which integrates all capacitances and resistances involved in each component. This simplified circuit provides a more practical representation of the input gas system. Only the humidifying system deserves a closer look since adding water vapor $Q_{m,\mathrm{vap}}$ into the dry gas flow $Q_{m,\mathrm{in}}$ changes the molar flow. However, estimating water vapor partial pressure at stacks input is crucial for voltage prediction. In its stationary state, a molar balance in the form exposed in the following equation:

$$Q_{\mathrm{hum,out}} = Q_{\mathrm{dry,in}} + Q_{\mathrm{vap}} \tag{10}$$

where

$$Q_{m,\mathrm{vap}} = f\left(Q_{\mathrm{dry,in}}, H_r, T\right) \tag{11}$$

occurs in the humidifying system. The evaporation flow which is represented by $Q_{m,\mathrm{vap}}$, is function of dry air flow, temperature and relative humidity level desired. Water vaporization rate $Q_{m,\mathrm{vap}}$ is modeled in the equivalent circuit by a current source, as shown in Fig. 5. Notice that in this figure, the Zenner diode represents vapor saturation pressure, introducing a nonlinear behavior to the model.

B. Fuel Cell Stack

Fuel cell gas circuits in the stack consist mainly in channels that can be modeled by an *RC* quadripole configuration. *RC* circuit parameters result from channel geometry and their disposition in the fuel cell stack.

As in the humidifying element, molar flow is not preserved in the stack. At the cathode, water vapor $Q^c_{m,\mathrm{vap}}$ is added to the air flow as a product of electrochemical reaction

$$Q_{m,\mathrm{H_2O},r} = \frac{nI_{\mathrm{stack}}}{2F} \tag{12}$$

electroosmotic drag

$$Q_{m,\mathrm{H_2O},e} = D * nI \tag{13}$$

and diffusion through the membrane

$$Q^m_{\mathrm{H_2O}} = Kd1\left([\mathrm{H_2O}^c_m] - [\mathrm{H_2O}^a_m]\right) + Kd2\left(P^c_{\mathrm{H_2O}} - P^a_{\mathrm{H_2O}}\right) \tag{14}$$

where from ideal gas law

$$P_{\mathrm{H_2O}} = \frac{RT}{V}\left(n_{\mathrm{H_2O}_m}\right) \tag{15}$$

and taking

$$[\mathrm{H_2O}_m] = \frac{n_{\mathrm{H_2O}_m}}{V} \tag{16}$$

From (15) and (16) we get

$$[\mathrm{H_2O}^c_m] = \frac{P_{\mathrm{H_2O}}}{RT}$$

and finally, (14) can be written as

$$Q^m_{\mathrm{H_2O}} = Kd\left(P^c_{\mathrm{H_2O}} - P^a_{\mathrm{H_2O}}\right) \tag{17}$$

with

$$Kd = Kd2 + \frac{Kd1}{RT}.$$

Nitrogen diffuses also according to pressure and concentration gradients, as shown for water in (14) and (17).

Nevertheless, a single *RC* circuit electric equivalent model is well adapted to describe a system where gases are treated as monocomponent gases, but it fails to predict gas composition and species partial pressure. The model presented this way is insufficient to represent adequately stack's general behavior. In order to describe internal partial pressure evolutions, gases in cathode and anode channels have to be decomposed into their elemental components. Each specie is considered as an ideal gas, and physical interactions between species are neglected. Under these considerations, cathode and anode are modeled by three independent circuits, one for each specie respectively.

Global pressure and flow at a given point "i" in each channel, are obtained by applying superposition properties to each individual gas circuit, according to gas composition in cathode and anode

$$\text{Cathode}\begin{cases} P^c(i) = \sum_k P^c_k(i), \\ Q^c_m(i) = \sum_k Q^c_{m,k}(i), \end{cases} \quad \text{for } k \in \{\mathrm{N_2}, \mathrm{O_2}, \mathrm{H_2O}\} \tag{18}$$

$$\text{Anode}\begin{cases} P^a(i) = \sum_k P^a_k(i), \\ Q^a_m(i) = \sum_{m,k} Q^a_{m,k}(i), \end{cases} \quad \text{for } k \in \{\mathrm{N_2}, \mathrm{H_2}, \mathrm{H_2O}\}. \tag{19}$$

When the system is decoupled into its different species, the reference pressure of the system cannot be the atmospheric

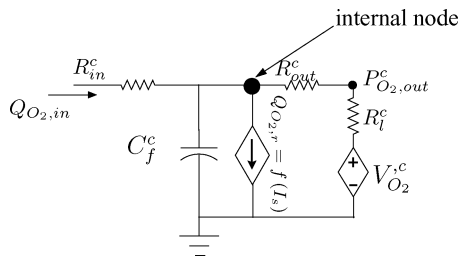

Fig. 6. Electric equivalent circuit for oxygen.

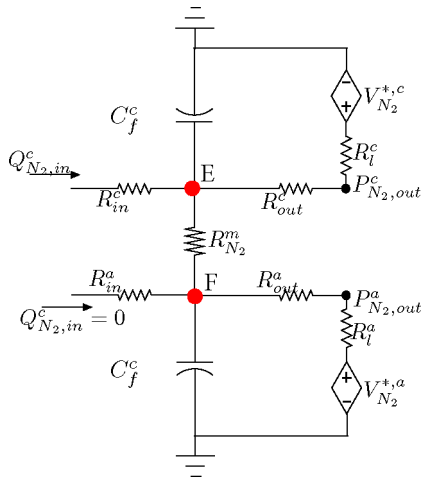

Fig. 7. Electric equivalent circuit for Nitrogen.

pressure any longer. In fact, independent species partial pressure is usually smaller than atmospheric pressure meaning (21)

$$\text{Cathode} \begin{cases} P_{\text{atm}} \leq P_{\text{N}_2} + P_{\text{O}_2} + P_{\text{H}_2\text{O}} \\ P_{\text{atm}} \geq P_{\text{N}_2}, P_{\text{O}_2}, P_{\text{H}_2\text{O}}. \end{cases} \tag{20}$$

$$\text{Anode} \begin{cases} P_{\text{atm}} \leq P_{\text{N}_2} + P_{\text{H}_2} + P_{\text{H}_2\text{O}} \\ P_{\text{atm}} \geq P_{\text{N}_2}, P_{\text{H}_2}, P_{\text{H}_2\text{O}}. \end{cases} \tag{21}$$

The modeling strategy is then to use absolute zero pressure as reference and to compensate each circuit output by a voltage (i.e., pressure) source V_{jk}, according to the following expression:

$$V^{*j}_k = \frac{P^j_{k,\text{out}}}{P^j_{\text{out}}} P_{\text{atm}} \tag{22}$$

to keep validity of (18) and (19), as shown in circuits Figs. 6–8. Notice that the circuit for hydrogen is analogous to oxygen circuit. If gas distribution at any cross section is supposed homogeneous, species flow will be proportional to its partial fraction at the given cross section. In this way, the output flow can be expressed by

$$Q^{a,c}_{m,k,\text{out}} = \frac{P_{k,\text{out}}}{P_{\text{out}}} Q_{m,\text{out}}, \qquad \text{for } k \in \{\text{N}_2, \text{H}_2, \text{H}_2\text{O}, \text{O}_2\}. \tag{23}$$

Considering (18)–(21) and (23), according to channel involved (cathode or anode) and considering (3) for the gas as a whole body, expression (22) can be deduced to estimate a voltage compensation source V_{jk} to be used in each specie circuit.

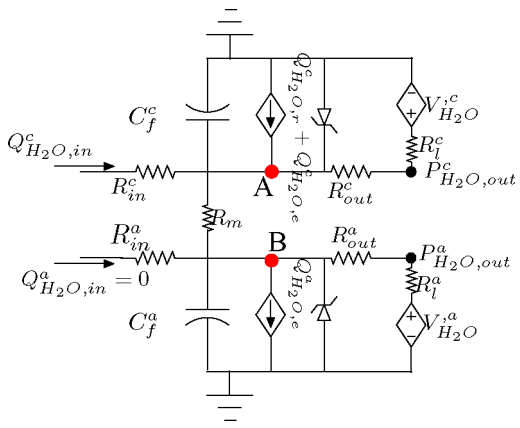

Fig. 8. Electric equivalent circuit for water vapor.

Assuming that no hydrogen and oxygen diffuse trough cells membrane, anode and cathode channels can be treated independently for these two species, resulting in the equivalent circuit proposed in Fig. 6, where the internal node voltage represents oxygen partial pressure. This circuit can be used either for oxygen or hydrogen, if resistances and capacitances are selected according to cathode or anode characteristics respectively. In the case of hydrogen and oxygen, gas consumption takes place due to electrochemical reaction. Oxygen and hydrogen gas molar consumption rates $Q_{\text{O}_2,r}$ and $Q_{\text{H}_2,r}$ are linear functions of the stack current. The actual relations for consumption rates are modeled in the circuit by current sources given by

$$\begin{aligned} Q_{k,r} &= \frac{NI}{\alpha F}, \qquad \text{for } k \in \{\text{H}_2, \text{O}_2\} \\ \alpha &= 2 \text{ for hydrogen} \\ \alpha &= 4 \text{ for oxygen} \end{aligned} \tag{24}$$

where N is the number of cells and α is the electron transfer ratio per reacted mole.

In the literature on modeling fuel cells, nitrogen diffusion is not considered as an important factor and its dynamics is not represented by the proposed models (see [6], [11], and [14]). In fact, under "open-mode" operating conditions, nitrogen migration effect is rather small. However, if the stack is set to operate in "close mode" (i.e., hydrogen out is closed in order to optimize fuel consumption), the assumption that hydrogen diffusion is negligible is no longer realistic. Indeed, nitrogen can be stored between flushes on the anode channels, leading an abnormal behavior. Hence, in this paper, the proposed model takes into account nitrogen diffusion. Notice that nitrogen and oxygen diffusion are ruled by the same gradient law presented in (17). Thus, both diffusion coefficients can be modeled by resistances that can either be taken as constants if a linearization near a working point is considered, or as variable resistances described as function of combined water activity on each side of membrane. Given the range of water activity found in stack normal operating conditions, nitrogen diffusion coefficient is assumed constant in a first approach. A resistance $R^m_{\text{N}_2}$ joining both anode and cathode *RC* circuits, models nitrogen diffusion

constant as shown in Fig. 7, where nodes E and F are internal nodes for partial pressure estimation.

Modeling water vapor requires additional considerations; phenomena like water production on cathode side and water migration from anode to cathode by electroosmotic drag (12), (13) are simultaneous to water diffusion from cathode to anode. Moreover, water vapor presents a saturation behavior, which limits its partial pressure to vapor saturation pressure at internal temperature and pressure conditions (see for instance [9])

$$P^{c,a}_{\mathrm{H_2O}} \leq P_{\mathrm{sat}}. \tag{25}$$

Finally, if the fuel cell operates with internal vapor pressures close to saturation pressure P_{sat}, the existence of liquid water inside the stack should also be considered. In this case, condensation evaporation phenomenon should also be included in the model. For the sake of simplicity, a first model considering only the influence of vapor phase water is developed in this paper.

Both electroosmotic water $Q_{m,\mathrm{H_2O},e}$ and produced water $Q_{m,\mathrm{H_2O},r}$ flows, described, respectively, by (12) and (13), are dependant of stack's current. They are modeled by current sources acting on corresponding channels. As in the case of nitrogen, a resistance linking the cathode and anode circuit, models water diffusion. Water diffusion and electroosmotic drag coefficients are dependent on membrane water content, which is usually estimated by water activity on either channel. The resulting electrical equivalent model is presented in Fig. 8, where nodes A and B are internal nodes for partial pressure estimation. When water partial pressure reaches its saturation level [9], the system is no longer linear. At this point, if net water flow is positive, liquid water is formed either as suspended particles or as liquid spots over channel surfaces, implying the need of adding a nonlinear component into the electrical equivalent model. In order to model vapor saturation pressure, a Zenner diode in parallel with the capacitance is introduced in the water equivalent circuit, to set a saturation voltage equivalent to vapor saturation pressure. In this way

$$V \leq V_{\mathrm{Zenner}} \tag{26}$$

as

$$P_{\mathrm{H_2O}} \leq P_{\mathrm{sat}}. \tag{27}$$

An integral function over the Zenner current allows estimating the amount of liquid water condensed in the fuel cell and its effect on stack voltage.

In order to complete the model, stack voltage model is built from open circuit voltage given by Nernst equation

$$E_{\mathrm{oc}} = E_o - \left[\frac{RT}{nF}\ln\frac{P_{\mathrm{H_2O}}}{P_{\mathrm{H_2}}\sqrt{P_{\mathrm{O_2}}}}\right] \tag{28}$$

with species partial pressures given by the equivalent voltages in the internal node of species circuits. Voltage losses under load conditions due to activation losses are described by Tafel's equation (see for instance [10])

$$v_{\mathrm{act}} = \left(\frac{RT}{\alpha nF}\right)\ln\left(\frac{i_0 + I}{i_0}\right) \tag{29}$$

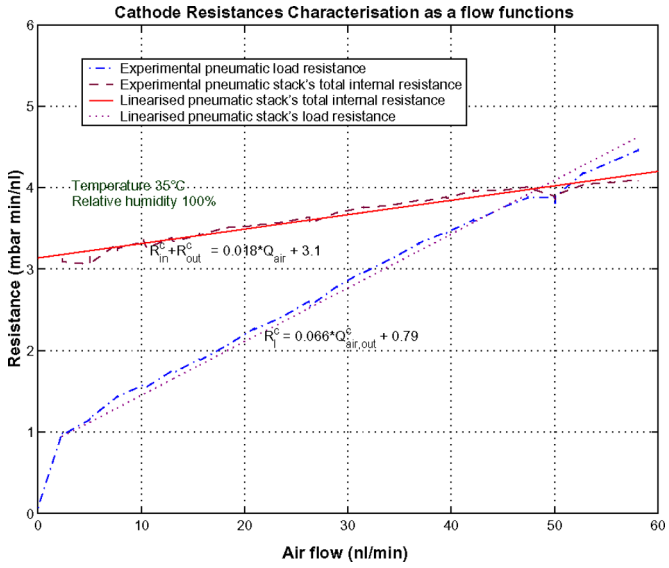

Fig. 9. Cathode load and internal resistances characterization.

concentration losses given by

$$v_{\mathrm{conc}} = \left(\frac{RT}{\alpha nF}\right)\ln\left(\frac{I_L - I}{I_L}\right) \tag{30}$$

and ohmic losses described by:

$$V_{\mathrm{Ohm}} = RI \tag{31}$$

are considered in the model.

C. Output Gas System

Output and input gas systems are generally alike, thus similar models can be constructed for both of them. However, its behavior is out of the scope of this paper and a simple load impedance $R^{a,c}_l$ will be used to model its influence on the stack. Moreover, this impedance is strongly linked to test bench facilities. For the sake of simplicity, in our case this impedance will be modeled by a variable load resistance, as shown in Figs. 6–8. Load resistance value is a function of gas flow as it can be observed in Fig. 9.

D. Global Model

If further precision or failure analysis is intended, the electrical model presented in the previous section can be insufficient to model cell behavior under extreme conditions, especially if diphasic water states (vapor, liquid) are expected to coexist in the stack. In this case when partial flooding occurs, calculated partial pressures in channels cannot serve as reactive site pressures any longer since a physical barrier (i.e., water film) will difficult and even block gas diffusion. In this case, three additional nodes should be considered: two nodes for reactional sites and another one for the membrane. In this way, a voltage difference between channels and reactional sites is allowed. Each reactive node will associate a capacitor modeling the diffusion layer volume, which is physically associated with electrode porosity. Single resistances will link the different nodes. Notice that resistances

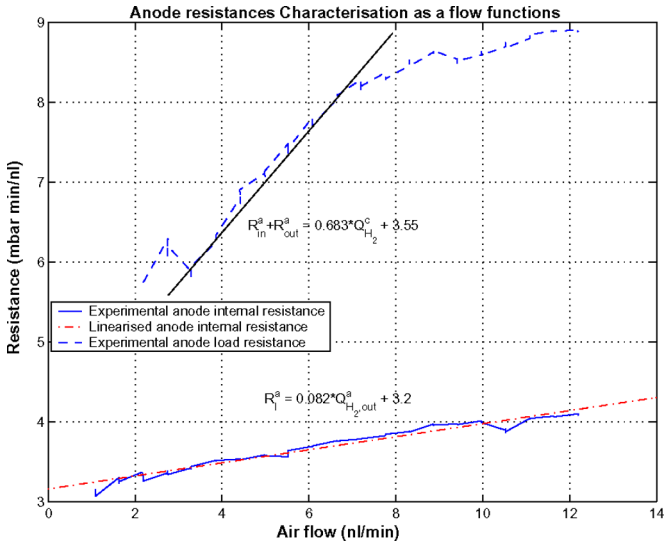

Fig. 10. Anode load and internal resistances characterization.

linking reactive nodes to channels and membrane nodes

$$R^{d,i}_{\min} \leq R^{d,i} \leq \infty \tag{32}$$

and

$$R^{m,i} = f(\lambda), \qquad \text{for } i = c, a \tag{33}$$

model diffusion phenomena and are considered to be variable, since an excess in liquid water will increase resistance. When flooding occurs, the value of the resistance is large enough to avoid gas exchange, leading to a voltage drop and even to a stack failure.

The equivalent circuits that model water vapor and oxygen including additional nodes are given, respectively, by Figs. 11 and 12, where voltage at nodes A, B, and C represent internal partial pressures. Hydrogen and nitrogen circuits are similar to oxygen and water vapor circuits, respectively.

V. Parameter Identification

Model parameter identification has been done in two steps. In a first step, anode and cathode circuits were decoupled experimentally by using dry gasses to feed the fuel cell stack. In this way, water vapor concentration between cathode and anode is small enough to neglect current through $R^m_{\mathrm{H_2O}}$, as shown in Fig. 8. Pneumatic input and output resistances in cathode and anode were calculated using (3), with data from tests done for different $Q^{a,c}_{\mathrm{gas,in}}$ and temperatures. As it is shown in [1] and [2], the pneumatic resistances in the model are not constant as proposed in similar models [5], [6]. In fact, for normal operation conditions, load and stack internal resistances can be represented as linear functions of gas flow. Results from those tests can be seen in Figs. 9 and 10. In Fig. 10, the load resistance associated to the test bench is linearized for low flow speeds where flooding is commonly found. Nonlinear behavior in load resistance is due to variable water content in exhaust gases.

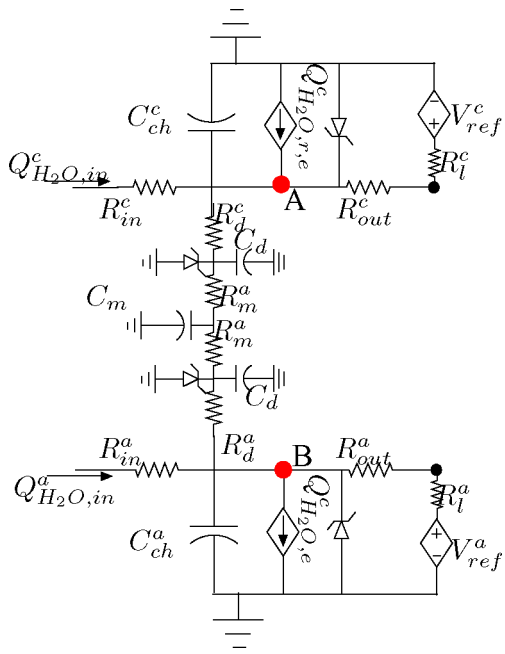

Fig. 11. Electric equivalent circuit for water vapor.

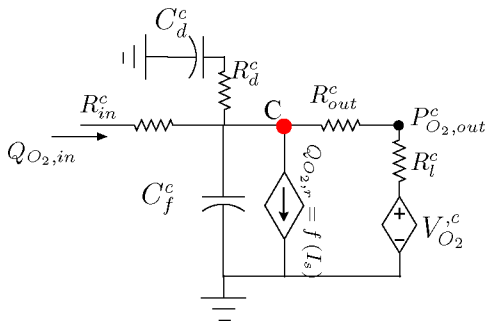

Fig. 12. Electric equivalent circuit for oxygen.

In a second step, cathode and anode circuit transfer functions were discretized and put in the following recurrence equation:

$$Y(i) = a \cdot Y(i-1) + b \cdot U(i). \tag{34}$$

Coefficients "a" and "b" in (34) are dependent of channel capacitance and pneumatic resistances. In this study, they are identified by a recurrent least square method on dynamic system tests. In a first approximation, input and output resistances are assumed to be identical. Using this method, the system is linearized around a given working point.

In a second approach, the nonlinear system with a varying resistance is treated. Resistance functions deduced from dry gas static tests shown in Figs. 9 and 10, are integrated to recurrence (34) to obtain capacitance values by recurrent least square method. Static tests were also driven with different humidity levels (different $Q^c_{\mathrm{H_2O,in}}$). The difference of circuit impedance between dry and humidified tests is assumed to be introduced by $R^m_{\mathrm{H_2O}}$ in Fig. 8 and used to identify $R^m_{\mathrm{H_2O}}$ in water equivalent circuit. In the global model (see Fig. 11), diffusion layer capacitances are obtained from (9) and estimated free volume

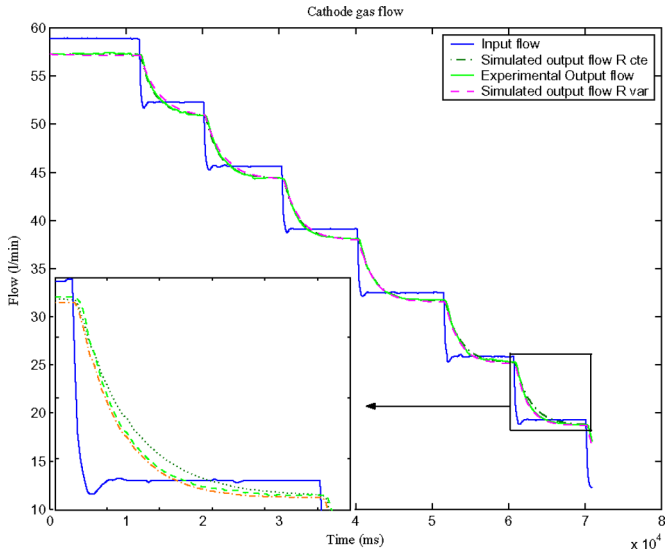

Fig. 13. Cathode flow simulation.

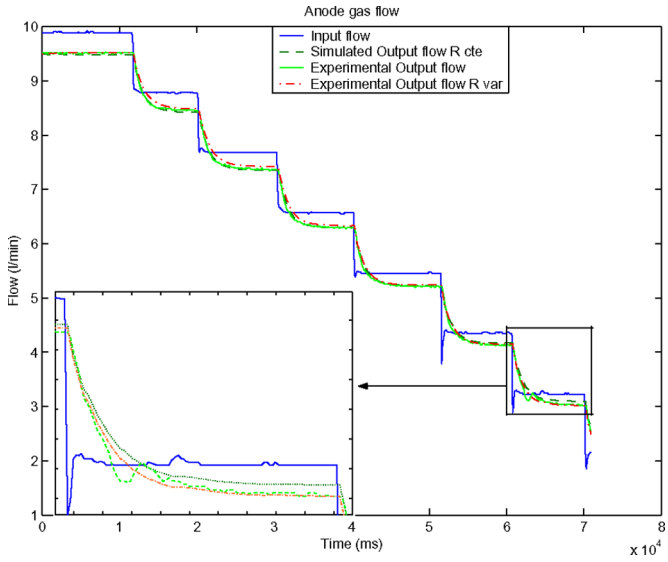

Fig. 14. Anode flow simulation.

in electrodes which is found using the equation

$$V = NPLHD \tag{35}$$

where N, P, L, H, and D design the number of electrodes, electrode porosity coefficient, electrode length, electrode height, and electrode depth, respectively.

Membrane capacitance models membrane capacity to store water λ_m and its relation to water activity am. An approximation for this capacitance can be obtained from water activity definition for Nafion117 (see [14]). Parameter values are optimized by using a recurrent least square method.

VI. Model Validation

The system used to carry out tests for model construction and validation, consists on a 500 W 20-cell stack and the associated test bench facility. Membrane humidification is ensured in our case by humidifying input air flow only. Air and hydrogen are taken from compressed gas cylinders and thus, gases are here considered unpolluted. Model simulation and experimental tests were driven under different experimental conditions to find model parameters [15] and to test model performances. Two different oxygen excess ratios and current profiles were chosen to test the model. Tests were developed under different water saturation, temperature and flow conditions.

Parameter validation was done using dynamic open circuit tests for varying gas flows, temperature, and input humidity levels.

In a first approach, constant resistance values were used. Figs. 13–15 show that the model is able to predict with a good approximation flow and pressure dynamics either at anode and cathode sides. Similar tests were used to observe model's performances in estimating Nernst voltage. Fig. 16 shows a good model estimation of open circuit voltage.

In a second approach, variable resistances are included in the model. It can be seen in Fig. 13 that even if model performances are acceptable with constant resistances, performances are considerably improved in a large flow range when using variable resistances. Thus, to obtain a more realistic model, variable resistances should be introduced to preserve good predictive abilities for a large range of gas flow conditions.

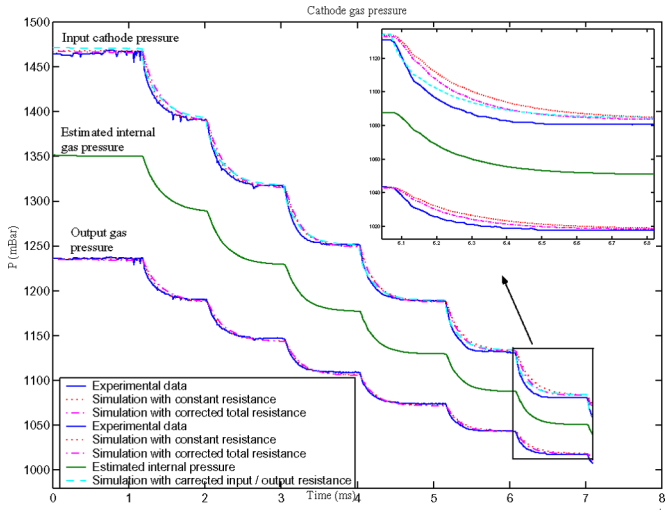

Fig. 15. Cathode pressure simulation.

The electric equivalent model of the fuel cell stack has been tested to simulate[1] output gas flow, output pressure and input pressure from a given gas input. It shows a good reproducibility of all parameter dynamics with small errors

1) $E_r^2\left(Q^c_{\text{out,air}}\right) \leq 9 \times 10^{-4}$ ln/min.
2) $E_r^2\left(Q^a_{\text{out,H}_2}\right) \leq 4 \times 10^{-4}$ ln/min
3) $E_r^2\left(P^c_{\text{out,air}}\right) \leq 1.7 \times 10^{-2}$ Pa
4) $E_r^2\left(P^a_{\text{out,H}_2}\right) \leq 1.4 \times 10^{-3}$ Pa
5) $E_r^2\left(P^c_{\text{in,air}}\right) \leq 1.4 \times 10^{-3}$ Pa
6) $E_r^2\left(P^a_{\text{in,H}_2}\right) \leq 1.4 \times 10^{-3}$ Pa
7) $E_r^2\left(v\right) \leq 1.3 \times 10^{-5}$ Pa

[1]Model simulation has been done using MATLAB. The use of specific electrical software as SABER and VHDL is in progress.

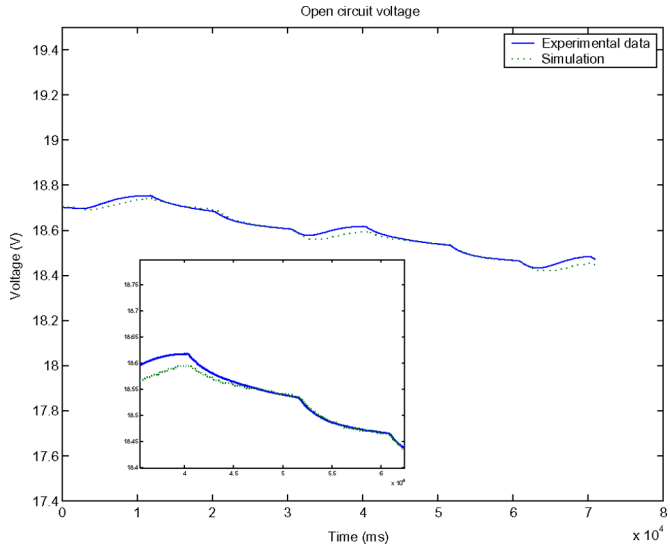

Fig. 16. Open circuit voltage simulation.

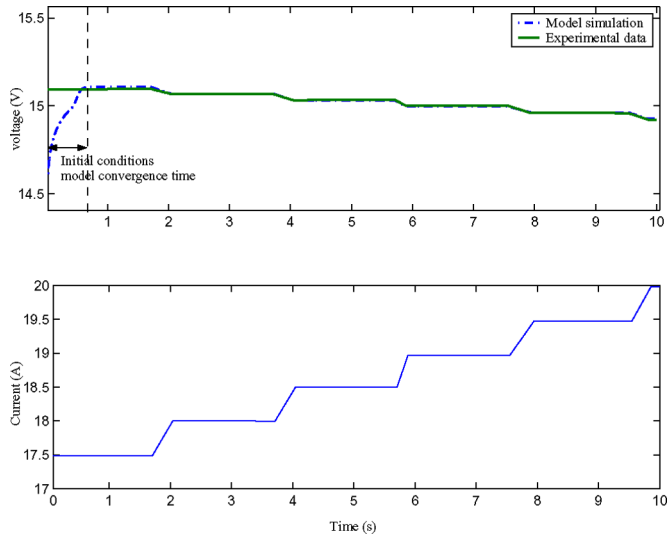

Fig. 17. Voltage simulation for step current profile.

where E_r denotes the relative error.

However, system time constant and gain are better preserved if variable resistances are used in the model.

Voltage estimation from partial pressures found by the electric equivalent model shows to fit well experimental results, for a large range of gas flow rates. Thus, partial pressure estimation by using the electrical equivalent circuit is valid for tested unsaturated water conditions in open circuit and in charge conditions, as it can be observed in Figs. 16 and 17.

VII. Diagnosis by Electrical Circuit Analysis

The electrical equivalent model representation presents characteristics that facilitates diagnosis for a PEFC.

1) First, the model can be easily linearized around the desired working condition, making possible observer utilization for residual generation. This is an important fact, since measurements inside the stack are rather difficult to obtain in real time, and the possibility of state reconstruction from the scare information available is highly desired.
2) Second, some failure modes can be associated with circuit parameters variation. A parametric approach to diagnosis such as Kalman filtering is then feasible.
3) As another advantage for this type of representation, we can take into account that existing software used for electrical network analysis, can easily be adapted.

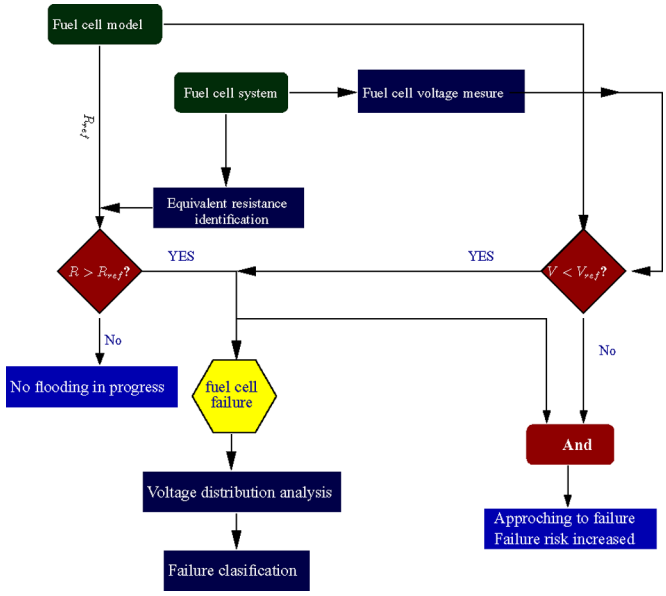

Fig. 18. Diagnosis algorithm.

A. Principal Failure Mode Description

In this paper, three main types of failures are considered.

1) Flooding.
2) Drying.
3) Membrane deterioration.

1) Flooding: The accumulation of liquid water in diffusion layer pores, and channel surfaces thus limiting gas exchange between channels and reactive sites, and between cathode and anode channels themselves, is called flooding. Flooding occurs mainly at the cathode side. It is the cumulative result of defective water management that can be summarized in three main causes.

1) Insufficient water evacuation flow.
2) Excess of input water vapor flow.
3) Sudden temperature drop.

Seen from another point of view, active surface is reduced producing an increase in current density, increasing also ohmic losses and decreasing fuel cell performance [1].

In the proposed model, flooding can be represented by simple variations in circuit parameters (see Fig. 19).

Water in its liquid state can partially limit gas flow through channels, increasing pressure losses between stacks input and output nozzles. This phenomenon can be represented in the circuit by an increase of input and output resistances. Gas diffusion can also be perturbed by the presence of liquid water. This perturbation is modeled by consequent variations of R_m

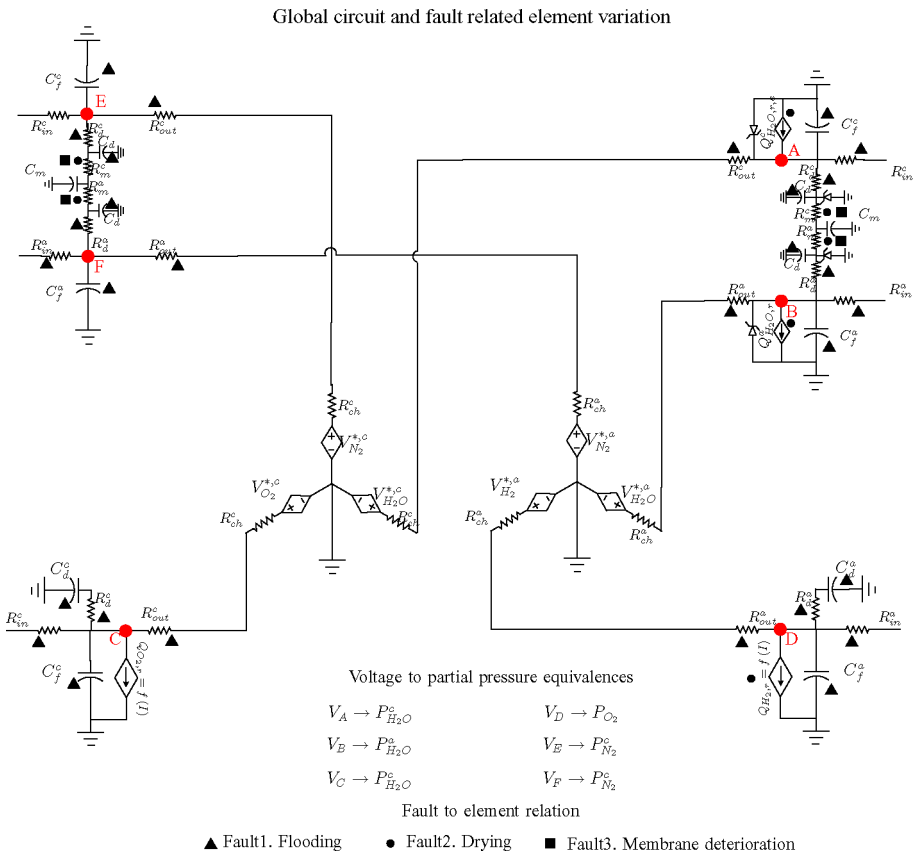

Fig. 19. System equivalent circuit and fault related elements.

in the circuit. In addition to water influence on circuit resistances, stored liquid water also leads to decrease the available gas volume. Since stack storage properties are modeled by a capacitance, this capacitance is also affected by liquid water production. Summarizing, flooding will produce the following changes in circuit parameters.

1) Increase in input and output resistances, specially at the cathode side.
2) Increase in R_m value, meaning decreasing gas diffusion rate.
3) Decrease of circuit capacitance due to reduced effective volume.

2) Drying: In opposition to flooding, drying occurs when water vapor balance is negative for a given time producing membrane dehydration. In a PEFC stack, proton transfer is assured by water molecules contained in the membrane. Membrane dehydration will increase electrical resistivity of the stack and will limit maximal current density and electroosmotic drag coefficient. Membrane width and thus gas diffusion constants will also be affected by dehydration. A decrease on R^m and a change on electroosmotic current source are expected.

Both, flooding and drying phenomena are transient conditions that can be reversed with an adequate control strategy, before a major failure occurs.

3) Membrane Deterioration: Membrane degradation takes place with time, and is considered as a permanent, nonreversible failure. Fuel cell performance is permanently compromized; it can be characterized by a system evolution toward new equilibrium points. As it can be easily inferred, only membrane parameters are affected in this case. Diffusion constants are significantly altered in most of the cases. Pressure gradient between cathode and anode channels drops, proportionally to failure magnitude. Under this consideration, R_m is expected to drop, but no other components should be altered.

B. Diagnosis Results

Failure tests presented in this article are conceived to carry the fuel cell stack onto a flooding failure mode. In order to flood the stack, two different strategies are used: an increase in input air humidity level and a stack temperature drop.

For variable relative humidity test, stack temperature was set to 50 °C and delivered current to 40 A for a constant gas flow. The fuel cell was initially set to initial conditions by operating it unloaded for 45 min at specified temperature and humidity conditions. Then, load is set to pull desired current and relative humidity level change function is set. An excess of water cumulates in the stack progressively presenting different effects.

Voltage degradation rate is constant as expected, since a direct relation between water content in the stack and voltage is supposed and given experimental conditions, a constant water formation rate is expected.

The relation between stack voltage degradation and flow resistance increase is observed in Fig. 20.

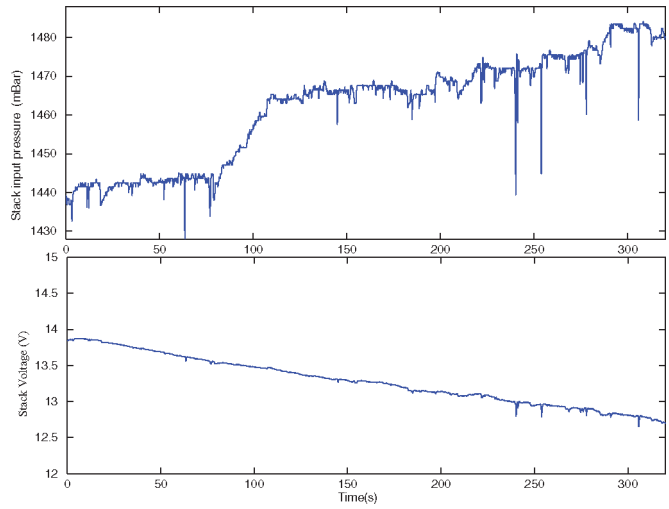

Fig. 20. Voltage degradation toward flooding fault mode at constant stack current and gas flow, due to an increase in humidity level.

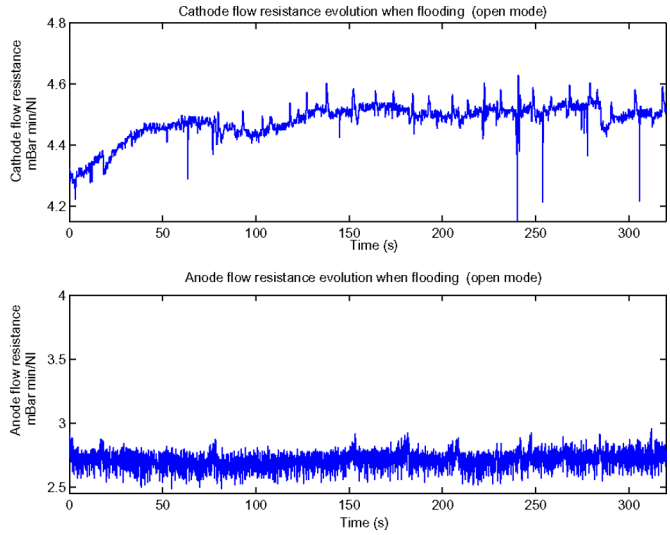

Fig. 21. Flow resistance evolution when flooding due to an increase in humidity level.

From the flow point of view, an increase on cathode flow resistance and cathode stack pressure loss is observed in the cathode whereas anode flow parameters remains relatively unchanged as expected. Experimental results illustrating previous phenomena are shown in Fig. 21.

Figs. 20 and 23 show that flooding is induced by a temperature drop or an increase in the input humidity level. In both cases, only cathode flow resistance is increased. However, a more continuous evolution of internal flow resistance is observed when reducing stack temperature, suggesting a more uniform water repartition in the stack. It is suggested that in order to distinguish between both flooding causes channel resistance parameter is insufficient and additional considerations should be taken into account.

Normally, pressure increase will produce an increase in voltage as described by the Nernst equation, however, experimental results in these tests show that a higher channel pressure is not

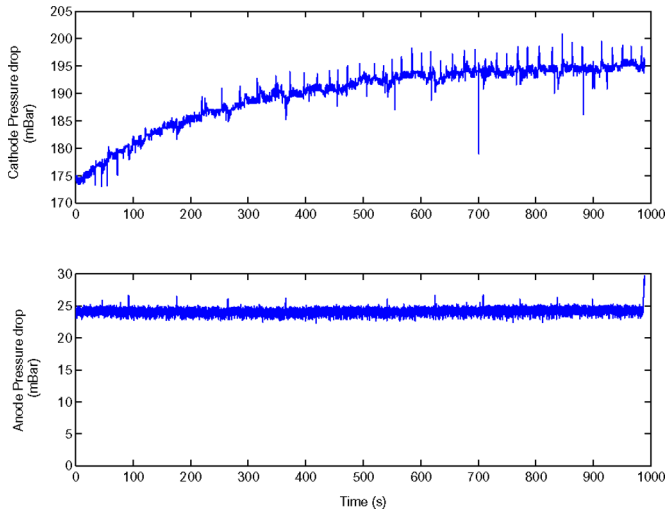

Fig. 22. Pressure losses evolution when flooding due to stack temperature decrease.

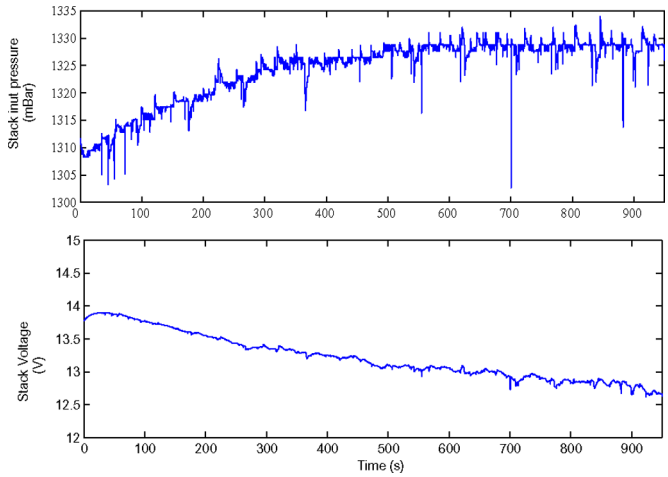

Fig. 23. Pressure and voltage evolution when flooding due to stack temperature decrease at constant stack current and gas flow.

necessarily related to a concentration increase on the reactional site. In fact, the obtained results suggest that diffusion resistances are increased when the stack floods as stated in the first section of this paper.

Diffusion resistance, channel resistance, evolution path, and cell voltage distribution shown in Fig. 24 are suggested as additional parameters to fine tune failure origin, since they are water distribution indicators in the stack.

A precise diffusion resistance identification was not possible due to indirect influence of variable air humidity on mass flow meter measurements, and a methodology to overcome this inconvenient will be subject of future studies.

VIII. Conclusion and Perspectives

In this paper, an electrical equivalent model of a PEFC which showed to be efficient in gas dynamic and voltage prediction has been developed. A diagnosis methodology based on the electrical circuit parameter identification has also been introduced.

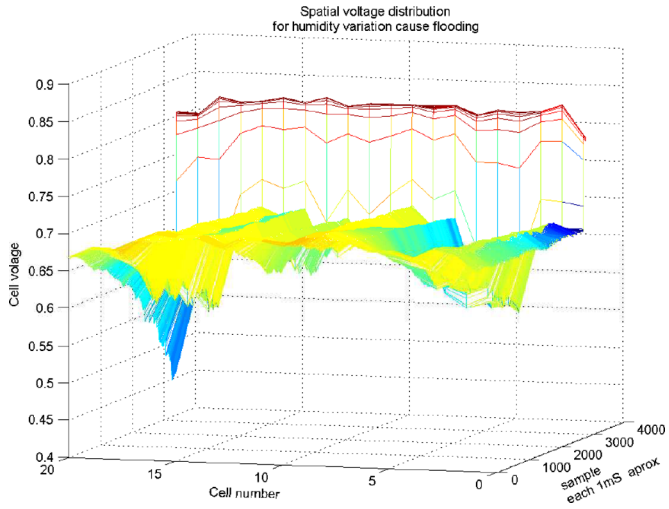

Fig. 24. Spatial voltage distribution evolution toward flooding failure.

Flow resistance shows clearly the presence on water excess in the stack, but it is insufficient to determine failure origin. Works are in progress in order to establish a model which takes into account saturated conditions to include liquid phase in the diffusion layer and to look at liquid water effect on circuit parameters. Results in this field are expected to give important information in fuel cell fault diagnosis.

Future studies will also be done to improve parameter identification methodologies, specially diffusion resistance estimation. Electric circuit parameter identification will be combined with flow resistance dynamics and cell voltage distribution to improve diagnosis performances.

APPENDIX

REFERENCE VALUES

Parameter estimation		
Parameter	**Unit**	Conditions
C_f^c	$0.05\,\frac{mole}{Pa}$	1
C_f^a	$0.03\,\frac{mole}{Pa}$	2
R_s^c	$0.018Q_{air}^c + 3.1\left[mbar * \frac{min}{l_n}\right]$	3
R_l^c	$0.066Q_{out}^c + 0.79\left[mbar * \frac{min}{l_n}\right]$	4
R_s^a	$0.683Q_{H2}^a + 3.55\left[mbar * \frac{min}{l_n}\right]$	5
R_l^a	$0.082Q_{out}^a + 3.2\left[mbar * \frac{min}{l_n}\right]$	6
$R_{H_2O}^m$	$2000\left[Pa\,\frac{s}{mole}\right]$	7
$R_{N_2}^m$	$5000000\left[Pa\,\frac{s}{mole}\right]$	8
Usefull constants		
R	3.3142	$\left[\frac{J}{K}\right]$
F	96485	$\left[\frac{C}{mole}\right]$
Pa	$1x10^{-5}$	$[bar]$

Conditions:
1) $T \approx 321\text{K}$
2) $T \approx 321\text{K}$
3) $T \approx 321\text{K}$
4) $T \approx 321\text{K}$
5) $T \approx 321\text{K},\ 3 \leq Q_{H2}^a \leq 7\left[\frac{l_n}{min}\right]$
6) $T \approx 321\text{K}$
7) $T \approx 321\text{K},\ \ H_r^c = 100\%$
8) $T \approx 321\text{K},\ H_r^c = 100\%$

REFERENCES

[1] A. Hernandez, D. Hissel, and R. Outbib, "Non linear state space modelling of a pemfc," *Fuel Cells Fundam. Syst.*, vol. 1, pp. 38–46, 2006.

[2] A. Hernandez, D. Hissel, and R. Outbib, "Electric equivalent model for a polymer electrolyte fuel cell (pemfc)," presented at the Electrimacs Conf, Hammamet, Tunisia, vol. 1, 2005, (ser. CD ROM).

[3] A. Jung, "A mathematical model of the hydrodynamical processes in the brain," in *Workshop Report II*. ed. Regensburg, Germany: N. und Nichtgleichgewicht in kondensierter Materie, 2002.

[4] T. Bourouina and J.-P. Grandchamp, "Modeling micropumps with electrical equivalent networks," *J. Micromech. Microeng.*, vol. 6, pp. 398–404, 1996.

[5] E. Hernandez and B. Diong, "A small-signal equivalent circuit model for pem fuel cells," in *Proc. 20th Annu. IEEE Appl. Power Electron. Conf. Expo.*, 2005, vol. 1, pp. 121–126.

[6] P. Famouri and R. S. Gemmen, "Electrochemical circuit model of a pem fuel cell," *Power Eng. Soc. Gen. Meeting*, vol. 3, pp. 1436–1440, 2003.

[7] S. Yu and S. Yuvarajan, "A novel circuit model for pem fuel cells," in *APEC 2004 Proc. (N. A. I. A. P. E. Conf. Expo., Eds.)*, vol. 1, pp. 362–366.

[8] A. Forrai, H. Funato, Y. Yanagita, and Y. Kato, "Fuel-cell parameter estimation and diagnostics," *IEEE Trans. Energy Convers.*, vol. 20, no. 3, pp. 668–675, Sep. 2005.

[9] *Asae—Psychometric Data*, ASAE D271.2, Dec. 1999.

[10] S. Yerramalla, A. Davari, A. Feliachi, and T. Biswas, "Modeling and simulation of the dynamic behavior of a polymer electrolyte membrane fuel cell," *J. Power Sources*, vol. 124, no. 1, pp. 104–113, 2003.

[11] J. T. Pukrushpan, H. Peng, and A. G. Stefanopoulou, "Control-oriented modeling and analysis for automotive fuel cell systems," *J. Dyn. Syst., Meas., Control*, vol. 126, no. 1, pp. 14–25, 2004.

[12] J. T. Pukrushpan, H. Peng, and A. G. Stefanopoulou, "Simulation and analysis of transient fuel cell system performance based on a reactant flow model," presented at the IMECE'02 (Int. Mech. Congr. Expo.), New Orleans, LA.

[13] R. Kerr *Fundamental Fluid Mechanics Lectures for es30a/d*, University of Warwick, 2005.

[14] T. Nguyen and R. White, "A water and heat management model for proton-exchange-membrane fuel cells," *J. Electrochem. Soc.*, vol. 140, pp. 2178–2186, Aug. 1993.

[15] F. Correa, J. M. Farret, J. Popov, and V. B. Parizzi, "Influence of the modelling parameters on the simulation accuracy of proton exchange membrane fuel cells," in *Power Tech. Conf. Proc. (IEEE Bologna Power Cell Conf.)*, 2003, vol. 2, 8 pp.

Andres Hernandez was born in Bogota, Colombia, in 1969. He received the Engineering degree from the Escuela Colombiana de Ingenieria, Bogota, Colombia, in 1997, and the Master's and Ph.D. degrees from the Université de Technologie de Belfort Montbéliard, Belfort, France, in 2003 and 2006, respectively.

From 1997 to 2002, he was a Lecturer at the Escuela Colombiana de Ingenieria. From 2006 to 2007, he was engaged in teaching and research activities as an ATER in the Université de Technologie de Belfort Montbéliard. Since 2007, he has been a Research Engineer in the Fuel Cell Systems Research Team, Laboratory of Electrical Engineering and Systems (L2ES), University of Franche-Comte, Belfort. His current research interests include fuel cell systems modeling and diagnosis.

Daniel Hissel (M'03–SM'04) was born in Boulay, France, in 1972. He received the Electrical Engineering degree from the Ecole Nationale Suprieure dIngnieurs Electriciens de Grenoble, Grenoble, France, in 1994, the Ph.D. degree from the Institut National Polytechnique de Toulouse, Toulouse, France, in 1998, and the Habilitation Diriger des Recherches from the University of Franche-Comte, Belfort, France, in 2004.

From 1999 to 2000, he was with ALSTOM Transport, Tarbes, France, where he was a System Engineer in electrical and fuel cell buses projects. From 2000 to 2006, he was an Associate Professor at the Laboratory of Electrical Engineering and Systems (L2ES). Since 2006, he has been a Full Professor at the University of Franche-Comte, where he is the Head of the Fuel Cell Systems Research Team, Laboratory of Electrical Engineering and Systems (L2ES). His current research interests include fuel cell systems dedicated to automotive applications, modeling, nonlinear control, energy optimization of these systems, and fuel cell system diagnosis.

Rachid Outbib was born in Casablanca, Marrocco, in 1962. He received the Ph.D. degree in applied mathematics from the University of Metz, Metz, France, in 1994, and the H.D.R. degree in automatics control from the University of Amiens, Amiens, France, in 1998.

From 2003 to 2006, he was a Full Professor at the University of Technology, Belfort, France. Since 2006, he has been a Full Professor at the University of Aix-Marseille II, Marseille, France. His current research interests include nonlinear systems methods with applications to fluid power and automotive applications.